Hypersonic band gap in an AlN-TiN bilayer phononic crystal slab

S. Hemon, Abdellatif Akjouj, A. Soltani, Yan Pennec, Y. El Hassouani, Abdelkrim Talbi, V. Mortet, Bahram Djafari-Rouhani

Hypersonic band gap in an AlN-TiN bilayer phononic crystal slab

Cite as: Appl. Phys. Lett. **104**, 063101 (2014); https://doi.org/10.1063/1.4864310
Submitted: 18 November 2013 • Accepted: 28 December 2013 • Published Online: 10 February 2014

S. Hemon, A. Akjouj, A. Soltani, et al.

Hypersonic band gap in an AlN-TiN bilayer phononic crystal slab

S. Hemon,[1] A. Akjouj,[1] A. Soltani,[1] Y. Pennec,[1] Y. El Hassouani,[2] A. Talbi,[3] V. Mortet,[4] and B. Djafari-Rouhani[1]
[1]*IEMN, UMR CNRS 8520, Université Lille 1, 59655 Villeneuve d'Ascq, France*
[2]*Department of Physics, Faculty of Science and Technology, University Moulay Ismail, Errachidia, Morocco*
[3]*LIA LICS/LEMAC - IEMN UMR CNRS 8520, ECLille, PRES Université Lille Nord de France, 59652 Villeneuve d'Ascq, France*
[4]*Institute of Physics of Academy of Sciences of Czech Republic, Fyzikalni AV CR, v.v.i., Na Slovance 1999/2, Czech Republic*

(Received 18 November 2013; accepted 28 December 2013; published online 10 February 2014)

We show both theoretically and experimentally the existence of a complete band gap in a phononic crystal (PnC) constituted by periodical air holes drilled in a solid bi-layer slab. The composite slab is formed with an aluminum nitride (AlN) layer deposited on a titanium nitride (TiN) thin metallic film. Indeed, AlN slabs are of great interest in many technological applications, in particular, owing to the capabilities of AlN as a complementary metal-oxide-semiconductor compatible material for integration in piezoelectric radio frequency filters (thin-film bulk acoustic resonator technology). The TiN layer was chosen as a buffer to enable small lattice mismatch with AlN, thus resulting in highly c-axis oriented and low stresses at the interface. We calculate the band structure of the crystal by using a finite element method and discuss the frequency and width of the band gap as a function of the thicknesses of both layers and the shape of the holes, i.e., from cylindrical to conical. The introduction of the TiN slab contributes to slowly widen the band gap. The band gap narrows when the holes become conical and closes when the radius of one face in the cone exceeds by 15% the radius of the other face. Experimentally, the measurement of the elastic wave transmission through eight rows of the bi-layer PnC shows a band gap around 950 MHz with an attenuation higher than 20 dB. The experimental results are well reproduced by the simulations provided the conical shape of the air inclusions is taken into account.
[http://dx.doi.org/10.1063/1.4864310]

Phononic crystals (PnCs) are heterogeneous materials which present a periodic modulation of their elastic properties.[1,2] Such materials open the way to new properties and functionalities not obtained using conventional bulk materials. One of the most interesting features is the existence of phononic band gaps (PBGs), in which the propagation of elastic waves is prohibited in a wide range of frequencies. PBGs can be used to realize fundamental functionalities in signal processing such as mirroring, guiding, filtering, and demultiplexing acoustic waves by the creation of defects in the PnC structure.[3] The possibility of implementation of these functionalities in the PnC structures can lead to integrated acoustic devices with high performance over the conventional electromechanical devices used in wireless communication and sensing systems.

While most of the earlier demonstrations of PBGs have been done in bulk[3–5] or surface acoustic wave[6–8] (SAW) phononic crystals, there is a growing interest in two-dimensional PnC slabs of finite thickness,[9–18] in particular, owing to the fact that acoustic waves remain confined in the slab and cannot escape into the vacuum, thus reducing considerably the losses through a substrate as in the case of SAW in 2D PnC structures. In addition to theoretical papers on the existence of complete PBGs in PnC plates,[9–11] experimental evidences of PBGs have been reported, first in the MHz range of frequency[12–14] and then more recently in the GHz regime.[15–18] Complete PBGs are of primary interest as they allow the complete engineering of the propagation of elastic waves in the PnC structure. Some defects such as linear waveguides have been introduced in perfect structures either along[19] or perpendicular[20,21] to the direction of propagation. Very recently, the confinement of elastic waves within a single defect in a phononic crystal slab[22] has been investigated both experimentally and theoretically. High frequency PnC structures are of considerable interest for compact wireless and sensing devices.

Among several material systems proposed for the fabrication of PnC plates, aluminum nitride (AlN) is of great interest due to its wide usage in electronic and photonic devices (for possible integration of electronic, photonic, and phononic functionalities).[17,18] In addition, AlN is a standard piezoelectric material to elaborate acoustic wave resonators and filters in radio frequency (RF) domain for mobile phones. In this Letter, we demonstrate theoretically the existence of a band gap in a PnC made of cylindrical air holes drilled in a solid bi-layer slab. The composite membrane is constituted of an AlN layer deposited on a thin titanium nitride (TiN) metallic film (see Fig. 1(a)). The thin film of TiN was chosen as the buffer layer due to the adaptation of the cubic cell (002) of AlN and (111) of TiN resulting in highly c-axis oriented and low stresses at the interface with AlN thin films. Moreover, metallic buffer allows achieving efficient transduction of symmetric Lamb wave modes for a wide range of operating frequencies. The thin film of TiN allows a high mechanical performance of the AlN membrane. The aim of this work is to investigate the effect of the geometrical parameters on the existence of absolute phononic band gaps, and to find the most suitable parameters

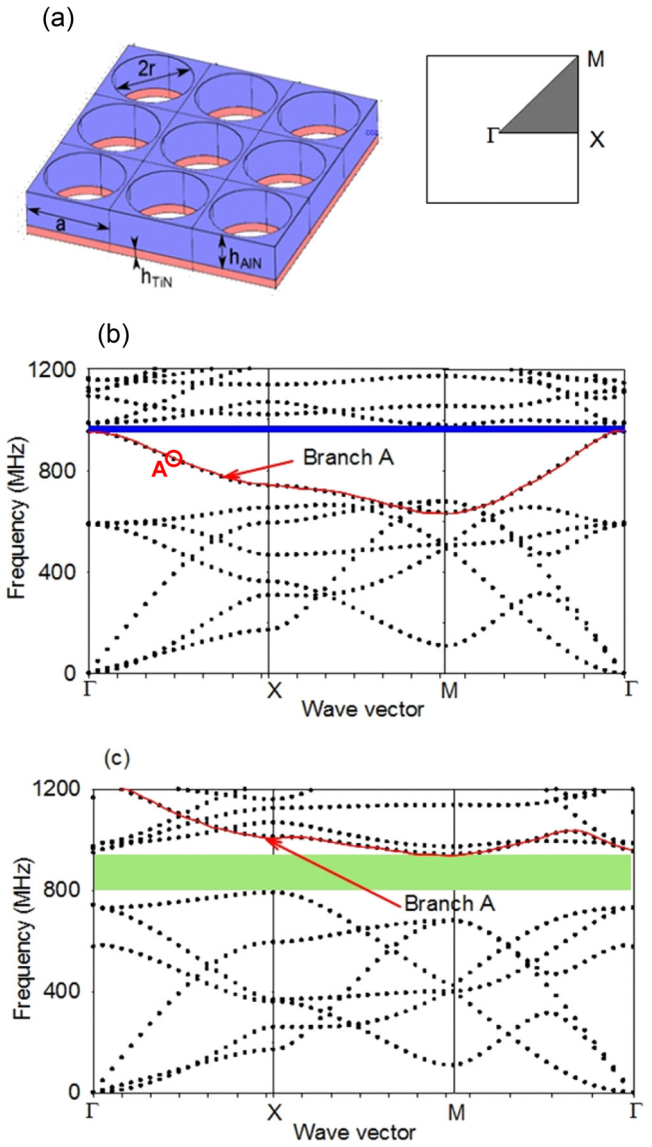

FIG. 1. (a) Bi-layer phononic crystal composed of AlN slab of thickness h_{AlN} deposited on a thin metallic TiN membrane of thickness h_{TiN}. Band structures of bi-layer AlN/TiN phononic crystal with $a = 4\,\mu$m, $h_{TiN} = 0.25\,\mu$m, $r = 1.84\,\mu$m, $f = 0.664$, and two different heights of AlN (b) $h_{AlN} = 2.8\,\mu$m and (c) $h_{AlN} = 1.6\,\mu$m.

that optimize the band gap width. We will discuss the relative effect of the thickness of each material (AlN and TiN) on the band gap width and central frequency. Since in the process of microfabrication the shape of the holes departs from cylindrical to conical, we also investigate the effect of the holes shape on the band structure. All numerical simulations are made with a finite element method (FEM).[23] The second part of the paper is devoted to the experimental evidence of a PBG in such bi-layer phononic crystal plate. We show that experimental results are in good agreement with the theoretical predictions of the PBG.

Figure 1(a) represents the phononic crystal plate composed of the two layers made respectively of AlN and TiN. The material properties of AlN and TiN used for the calculations are reported in Table I. The bi-layer is drilled with cylindrical air holes arranged in a square array. In the following, the thickness of AlN is denoted h_{AlN} and the thickness of TiN h_{TiN}. Besides the thicknesses, the other geometrical

TABLE I. Material properties of AlN and TiN used for the calculations.

Properties\materials	AlN (hexagonal)	TiN (cubic)
C_{11} (10^9 N/m^2)	396	610
C_{12} (10^9 N/m^2)	137	100
C_{13} (10^9 N/m^2)	108	100
C_{33} (10^9 N/m^2)	373	610
C_{44} (10^9 N/m^2)	121	168
C_{66} (10^9 N/m^2)	130	168
ρ (kg/m^3)	3255	5390

parameters are the lattice parameter a and the radius of the inclusion r, resulting in a filling fraction of the composite medium defined as the ratio $f = \pi r^2/a^2$. For all calculations, we took a lattice parameter a equal to 4 μm which corresponds to the experimental lattice pitch of the crystal described in the second part of the paper.

Before discussing the existence and behavior of the band gap as function of the layer thicknesses, the following two remarks are worth being noticed. Previous works dealing with phononic crystal slabs made of a single material drilled periodically with holes[9,11] have shown that the band gap opens only when the thickness of the slab is around half of the lattice period. It closes for a very small thickness as well as when the thickness goes above the lattice period. More precisely, the band gap results from the overlap of two partial band gaps associated with modes which are respectively symmetric and anti-symmetric with respect to the middle plane of the slab. Generally, the latter gap is narrower and contains the former, so the edges of the complete band gap are constituted by two anti-symmetric branches. Such trends will be also obtained below for the bilayer structure studied in this paper. The second remark is that in our case of AlN-TiN bilayer, the thickness of TiN is in general much smaller than that of AlN because the former has essentially the role of a buffer layer in practical fabrication processes.

Figures 1(b) and 1(c) represent the calculated dispersion curves along the three high symmetry directions of the irreducible Brillouin zone ΓX, ΓM, and XM for two sets of parameters. In the first calculation (Figure 1(b)), we took a set of parameters closed to those of the experimental device investigated in the second part of the paper. The thicknesses of the layers are, respectively, $h_{AlN} = 2.8\,\mu$m and $h_{TiN} = 0.25\,\mu$m while the radius of the cylinders is equal to $r = 1.84\,\mu$m. With these parameters, the dispersion curve shows clearly the existence of a small absolute phononic band gap of width 50 MHz around 955 MHz (see the shaded blue area in Fig. 1(b)). In the second calculation (Figure 1(c)), we kept the same parameters as before except the thickness of the AlN plate which takes now the value of $h_{AlN} = 1.6\,\mu$m. The impact of a thinner AlN plate has been to increase the width of the band gap to 170 MHz around 860 MHz. The widening of the band gap essentially comes from the quick shift of one specific branch (highlighted in red and labeled A in Figs. 1(b) and 1(c)) towards the high frequencies as compared to the general shift of the other dispersion branches. To give a deeper insight about the origin of branch A, we have calculated the three components of the displacement field for a point belonging to this branch at the middle of the ΓX direction of the Brillouin zone (Figure 2). One can see that mode A is mainly "in-plane,"

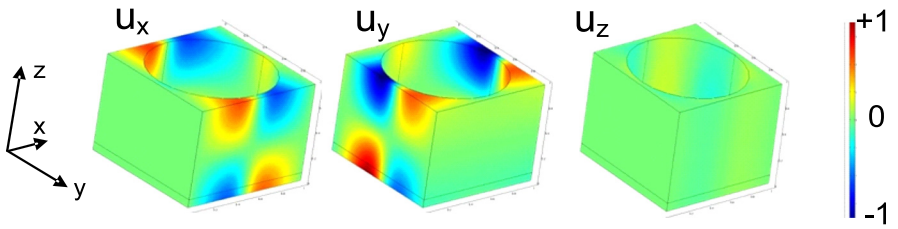

FIG. 2. Maps of the displacement field components at point A of Figure 1(b).

which means that the components of the displacement field are in the (x, y) plane and anti-symmetric with respect to the middle plane of the slab. The calculations of the displacement fields have been performed for the lowest six branches and branch A. We found that the first five branches correspond to fundamental modes, either in plane and symmetric or out of plane and antisymmetric and therefore present a displacement field which is uniform along the thickness of the plate. On the contrary, branch 6 as well as branch A are both in plane and antisymmetric, resulting in a non uniform distribution of the displacement field along the thickness of the plate as shown in Fig. 2. This analysis shows that an increase of the plate thickness results in a quicker frequency shift of branches 6 and A in comparison to the other branches, thus leading to the widening of the band gap width. Finally, it is worthwhile noticing that in Fig. 1(b) branch A presents a negative slope around the Γ point that could be useful for negative refraction applications.

Figure 3(a) shows the evolution of the band gap edges as a function of the thickness h_{AlN} keeping constant the TiN thickness ($h_{TiN} = 0.25\,\mu$m). The band gap opens when the thickness of AlN reaches 0.6 μm, then the band gap width (green area) increases and reaches a maximum for $h_{AlN} = 1.6\ \mu$m before decreasing until the band gap closes at $h_{AlN} = 2.4\,\mu$m. The closing of the gap results again from a faster downwards shift of branch A than the other branches. The band gap remains closed from $h_{AlN} = 2.4$ to 2.6 μm, but a new band gap opens above the branch A when h_{AlN} exceeds 2.6 μm (blue area in Fig. 3(a)). As a partial conclusion, the existence, width, and central frequency of the band gap are mainly governed by the position of the branch A and the maximum band gap width of 170 MHz is obtained for $h_{AlN} = 1.6\,\mu$m at 860 MHz. In order to understand the effect of the additional TiN layer, we have also presented in Fig. 3(a) (dashed lines) the evolution of the band gap for a slab constituted of AlN material only. One can conclude that while the general behavior is almost the same, the introduction of the TiN layer increases the band gap by almost 20% for h_{AlN} between 1.35 and 1.85 μm. One can also notice that for h_{AlN} between 1.85 and 2.8 μm, the shift of branch A towards lower frequencies is faster in the bi-layer slab than in the homogeneous AlN one.

Figure 3(b) shows the evolution of the band gap width as a function of h_{TiN}, keeping h_{AlN} as a constant, for the following set of geometrical parameters: $a = 4\,\mu$m, $r = 1.84\,\mu$m ($f = 0.665$), and $h_{AlN} = 1.6\,\mu$m. Figure 3(b) shows that an optimization of the band gap width is obtained for a TiN thickness of $h_{TiN} = 0.25\,\mu$m. Figure 3(c) sketches the evolution of the band gap width as a function of h_{TiN}, keeping $h_{PnC} = h_{AlN} + h_{TiN}$ as a constant, for a same filling factor. One can see that whatever is the distribution of the AlN and TiN thicknesses, the band gap width is almost constant. This result supports again the idea that the main geometrical parameter is the total thickness of the slab as compared to the

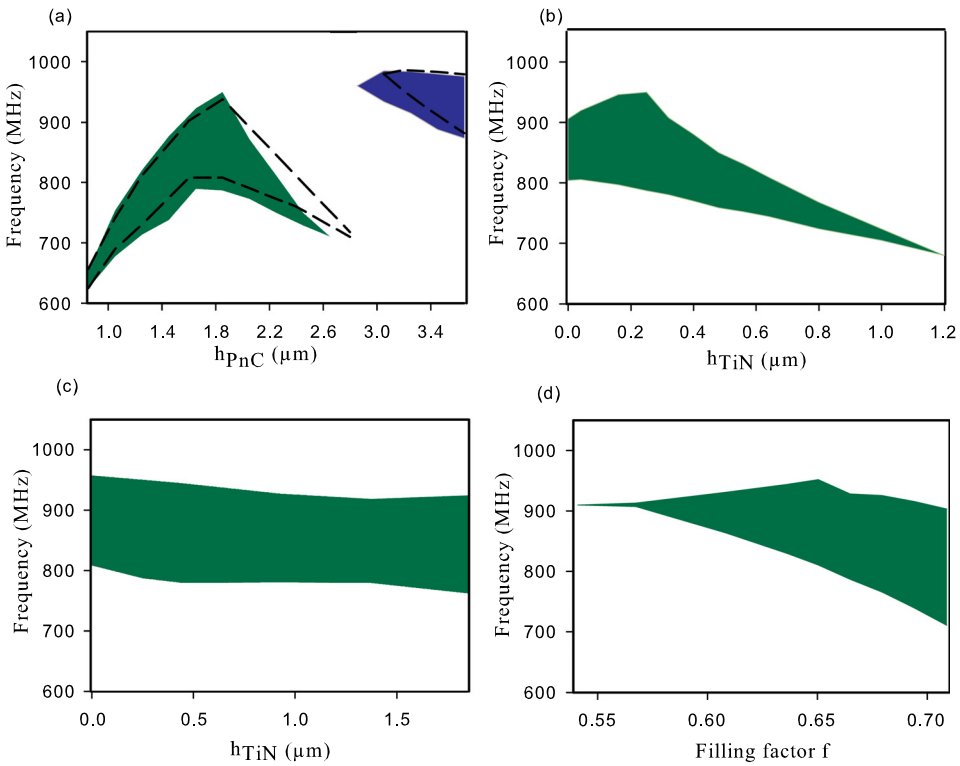

FIG. 3. (a) Evolution of the width of the gap (green area) as a function of the thickness h_{PnC} of the phononic crystal (AlN + TiN bi-layer) with $a = 4\,\mu$m, $h_{TiN} = 0.25\,\mu$m, and $r = 1.84\,\mu$m. The dashed lines represent the band gap boundaries in an equivalent single-layer slab of AlN thickness. (b) Evolution of the width of the band gap vs the thickness of the TiN layer, for $h_{AlN} = 1.6\,\mu$m, $a = 4\,\mu$m, and $f = 0.664$. (c) Evolution of the width of the band gap vs the thickness of the TiN layer, for $h_{PnC} = h_{AlN} + h_{TiN} = 1.85\,\mu$m, $a = 4\,\mu$m, and $f = 0.664$. (d) Width of the band gap as a function of the filling fraction, calculated for $a = 4\,\mu$m; $h_{TiN} = 0.25\,\mu$m and $h_{AlN} = 1.6\,\mu$m.

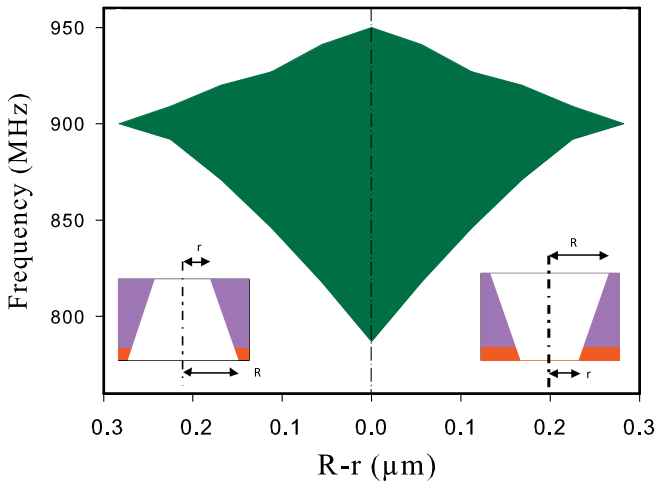

FIG. 4. Evolution of the width of the band gap as a function of R-r, for $a = 4\,\mu$m, $R = 1.84\,\mu$m, $h_{AlN} = 1.6\,\mu$m, and $h_{TiN} = 0.25\,\mu$m. The x-axis is given by the difference between the constant radius R and the variable radius r of the conical hole.

lattice period. However, it should be noticed that the materials considered here have relatively close velocities whereas different trends can be obtained for other choices of the materials in the bilayer having very different velocities. Finally, keeping constant the thicknesses of the two layers ($h_{TiN} = 0.25\,\mu$m and $h_{AlN} = 1.6\,\mu$m), we show in Fig. 3(d) the behavior of the band gap as a function of the filling fraction. We note the existence of a complete band gap over a large range of filling fraction above 0.55. The width of this gap increases continuously until the close packing is reached in the crystal, as already reported in the literature.[9,11]

Until now, we have assumed that the holes have a perfect cylindrical shape. However, in the process of microfabrication, the holes display most of the time a conical shape with a small angle. Therefore before going to the experimental results, we discuss the effect of this conic shape on the phononic band gap. All the calculations are made with the following parameters: $a = 4\,\mu$m, $h_{AlN} = 1.6\,\mu$m, and $h_{TiN} = 0.25\,\mu$m, which provide an optimal bandwidth of the gap. We take the radius R of the circle on one side of the cone equal to $1.84\,\mu$m and calculate the band structure by varying the radius r of the circle on the opposite face of the cone. As schematically represented in the inset of Fig. 4, two configurations are considered, namely, the constant radius R on the top or on the bottom side of the bi-layer phononic slab. In Fig. 4, we report the evolution of the band gap edges as a function of the difference $(R\text{-}r)$. The larger band gap is obtained for the cylindrical shape of the holes and the band gap closes as far as the smallest radius in the cone (either on top or at the bottom face) reaches $1.54\,\mu$m, which means a difference of 15% with respect to R.

In the last part of this work, we present an experimental result obtained for a bi-layer TiN/AlN phononic crystal. As reported above, the (TiN) thin film was chosen as a buffer layer because of its low electrical resistivity, and small lattice mismatch between AlN (002) and (111) cubic TiN. First, the magnetron plasma discharge parameters were optimized to obtain well crystallized AlN thin films with less than 0.4% oxygen contamination. The transmission electronic microscopy analysis shows AlN thin film deposited on (100) silicon (not shown here) highly oriented close to the AlN surface only. It presents a rocking curve which can reach 1.2° for optimized thin films. Low intrinsic stress (111) cubic TiN films deposited on (100) silicon substrate were obtained by RF sputtering at low temperature (<200 °C) followed by a annealing under vacuum. This annealing improves the crystal orientation of TiN and favors (111) TiN planes. The diffraction peak is observed at 36.7° and is indexed as cubic (111) TiN planes which is close to the hexagonal (002) AlN localized at 36°. Finally, a successful deposition of highly oriented AlN thin film at low temperature on a TiN buffer layer is obtained.

We then proceed to the characterization of the bi-layer phononic crystal considering the guided acoustic waves was lunched and detected using interdigital transducers (IDTs) (emitter and receiver) as shown in the inset of Fig. 5. The characterized SAW filter presented here is the device realized with IDTs patterned with $4\,\mu$m finger resolution. This IDT resolution involves the wavelength λ of $16\,\mu$m. Figure 5 shows the scanning electron microscope images of a top view and a cross section of the sample. The measure gives the following set of parameters: $a = 4\,\mu$m, $h_{AlN} = 2.8\,\mu$m, $h_{TiN} = 0.25\,\mu$m, R (upper radius) $= 1.8485\,\mu$m, r (lower radius) $= 1.7355\,\mu$m. The conical shape of the hole can then be characterized by the relative variation $(R\text{-}r)/R = 5\%$. To record the band gap properties of the fabricated PnCs, we monitored the transmission in the ΓX direction through a phononic structure containing eight periods of holes. We

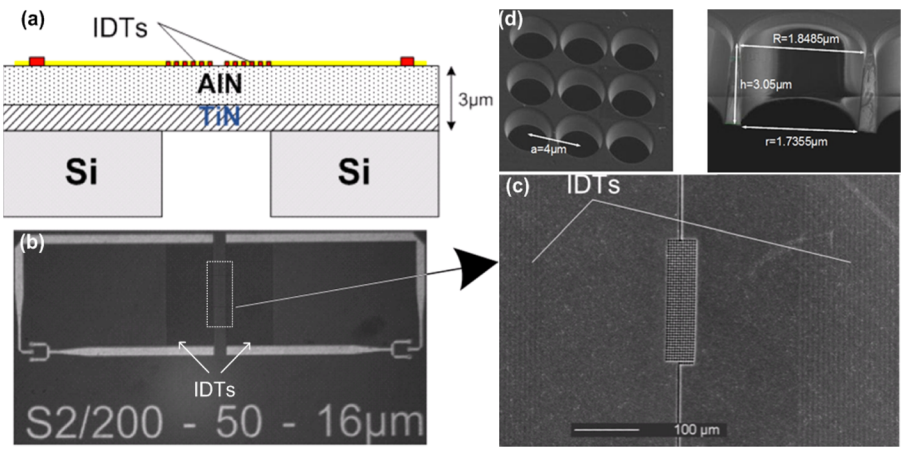

FIG. 5. (a)–(c) Experimental setup. (d) Scanning electron microscopy of (left) the fabricated square lattice PnC structure and (right) the cross section through one conical shape hole.

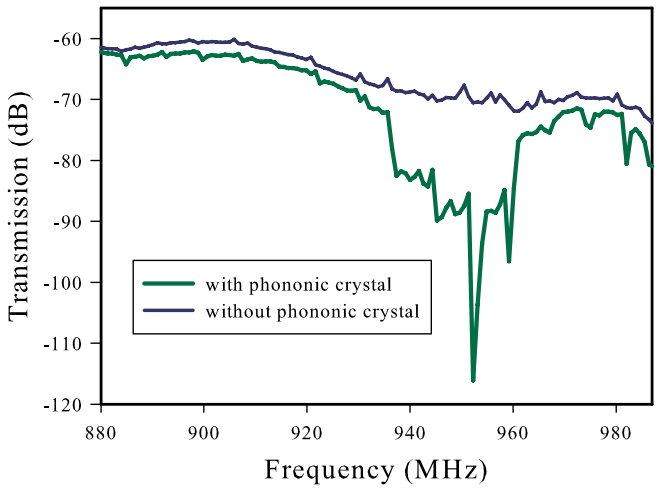

FIG. 6. Experimental transmission through the PnC structure shown in Fig. 5 as a function of frequency. The length of the PnC structure between the two electrode structures is eight layers.

used a network analyzer to excite the structure, applying a high frequency electrical signal between the first and the second layer of metal producing an electric field across the AlN layer.

All the devices were electrically characterized with an Agilent 8752 A network analyzer using 125 μm pitch G-S-G probes. Figure 6 shows the frequency response of this SAW device with and without PnC. Over the monitoring frequency range, a wide window of low transmission reduced by more than 20 dB appears in the range [935, 962 MHz]. To obtain theoretically this central frequency with cylindrical holes, it is necessary to assume a radius of the cylinders equal to 1.855 μm, i.e., 3% larger than the average experimental radius. On the other hand, to reproduce theoretically the experimental bandwidth, we need to assume a conical shape of the hole with a relative variation of $(R\text{-}r)/r = 5\%$, i.e., the value corresponding to the measurements.

In summary, the purpose of this paper was to investigate a bi-layer phononic crystal plate drilled with air holes and made with two constituents AlN and TiN. For a plate made of one material, we know from the literature[9,11] that a large band gap can be obtained when the thickness of the plate is about half of the PnC lattice parameter. The introduction of a thin metallic layer (TiN) as a support of the AlN membrane for the purpose of technological applications can significantly widen the gap bandwidth by almost 20% for a PnC whose thickness is between 1.35 and 1.85 μm. We show that the opening of a band gap in the bi-layer phononic slab is largely due to the quick shift of one specific branch which moves faster than the other dispersion curves as a function of the thickness of the plate due to symmetry considerations. We also investigated the effect of the conical shape of the holes on the band structure and found that a relative variation of $(R\text{-}r)/R = 15\%$ closes definitely the band gap. Finally, we measured the experimental transmission spectrum along the ΓX direction of a fabricated sample formed by etching air holes in a bi-layer solid. The experimental result is well reproduced by the simulations provided we take account of the conical shape of the holes.

Y.P. and B.D.R. would acknowledge the support of the project Metactif, provided by the Agence Nationale de la Recherche and Direction Generale de l'Armement under grant ANR-11-1STR-015. V. M. is a J. E. Purkyne (ASCR) research fellow.

[1]M. S. Kushwaha, P. Halevi, L. Dobrzynski, and B. Djafari-Rouhani, Phys. Rev. Lett. **71**, 2022 (1993).
[2]M. M. Sigalas and E. N. Economou, Solid State Commun. **86**, 141 (1993).
[3]Y. Pennec, J. O. Vasseur, B. Djafari-Rouhani, L. Dobrzynski, and P. A. Deymier, Surf. Sci. Rep. **65**, 229 (2010).
[4]J. V. Sanchez-Perez, D. Caballero, R. Martinez-Sala, C. Rubio, J. Sanchez-Dehesa, F. Meseguer, J. Llinares, and F. Galvez, Phys. Rev. Lett. **80**, 5325 (1998).
[5]F. R. Montero de Espinoza, E. Jimenez, and M. Torres, Phys. Rev. Lett. **80**, 1208 (1998).
[6]Y. Tanaka and S. I. Tamura, Phys. Rev. B **58**, 7958 (1998).
[7]A. Khelif, Y. Achaoui, S. Benchabane, V. Laude, and B. Aoubiza, Phys. Rev. B **81**, 214303 (2010); Y. Achaoui, A. Khelif, S. Benchabane, L. Robert, and V. Laude, *ibid.* **83**, 104201 (2011); A. Khelif, Y. Achaoui, and B. Aoubiza, J. Appl. Phys. **112**, 033511 (2012).
[8]F. Meseguer, M. Holgado, D. Caballero, N. Benaches, J. Sanchez-Dehesa, C. Lopez, and J. Llinares, Phys. Rev. B **59**, 12169 (1999).
[9]A. Khelif, B. Aoubiza, S. Mohammadi, A. Adibi, and V. Laude, Phys. Rev. E **74**, 046610 (2006).
[10]J. H. Sun and T. T. Wu, Phys. Rev. B **76**, 104304 (2007).
[11]J. O. Vasseur, P. A. Deymier, B. Djafari-Rouhani, Y. Pennec, and A. C. Hladky-Hennion, Phys. Rev. B **77**, 085415 (2008).
[12]X. Zhang, T. Jackson, E. Lafond, P. Deymier, and J. Vasseur, Appl. Phys. Lett. **88**, 041911 (2006).
[13]S. Mohammadi, A. A. Eftekhar, A. Khelif, H. Moubchir, R. Westafer, W. D. Hunt, and A. Adibi, Electron. Lett. **43**, 898 (2007).
[14]N.-K. Kuo, C. Zuo, and G. Piazza, Appl. Phys. Lett. **95**, 093501 (2009).
[15]M. F. Su, R. H. Olsson III, Z. C. Leseman, and I. El-Kady, Appl. Phys. Lett. **96**, 053111 (2010).
[16]Y. M. Soliman, M. F. Su, Z. C. Leseman, C. M. Reinke, I. El-Kady, and R. H. Olsson III, Appl. Phys. Lett. **97**, 193502 (2010).
[17]M. Gorisse, S. Benchabane, G. Teissier, C. Billard, A. Reinhardt, V. Laude, E. Defaÿ, and M. Aïd, Appl. Phys. Lett. **98**, 234103 (2011).
[18]N.-K. Kuo and G. Piazza, Appl. Phys. Lett. **99**, 163501 (2011).
[19]F. L. Hsiao, A. Khelif, H. Moubchir, A. Choujaa, C. C. Chen, and V. Laude, Phys. Rev. E **76**, 056601 (2007).
[20]S. Mohammadi, A. A. Eftekhar, W. D. Hunt, and A. Adibi, Appl. Phys. Lett. **94**, 051906 (2009).
[21]C.-Y. Huang, J.-H. Sun, and T.-T. Wu, Appl. Phys. Lett. **97**, 031913 (2010).
[22]R. Marchal, O. Boyko, B. Bonello, J. Zhao, L. Belliard, M. Oudich, Y. Pennec, and B. Djafari-Rouhani, Phys. Rev. B **86**, 224302 (2012).
[23]M. Aberg and P. Gudmundson, J. Acoust. Soc. Am. **102**, 2007 (1997).